CHEMISTRY
A EUROPEAN JOURNAL

Electronic Structural Changes between Nickel(II)–Semiquinonato and Nickel(III)–Catecholato States Driven by Chemical and Physical Perturbation

Hideki Ohtsu and Koji Tanaka*[a]

Abstract: The selective synthesis of tetracoordinate square-planar low-spin nickel(II)–semiquinonato (Ni^{II}-SQ) and nickel(III)–catecholato (Ni^{III}-Cat) complexes, **1** and **2**, respectively, was achieved by using bidentate ligands with modulated nitrogen-donor ability to the nickel ion. The electronic structures of **1** and **2** were revealed by XPS and EPR measurements. The absorption spectra of **1** and **2** in a noncoordinating solvent, dichloromethane (CH_2Cl_2), are completely different from those in tetrahydrofuran (THF), being a coordinating solvent. As expected from this result, the gradual addition of *N*,*N*-dimethylformamide (DMF), which is also a coordinating solvent like THF, into a solution of **1** or **2** in CH_2Cl_2 leads to color changes from blue (for **1**) and brown (for **2**) to light green, which is the same color observed for solutions of **1** or **2** in THF. Furthermore, the same color changes are induced by varying the temperature. Such spectral changes are attributable to the transformation from square-planar low-spin Ni^{II}-SQ and Ni^{III}-Cat complexes to octahedral high-spin Ni^{II}-SQ ones, caused by the coordination of two solvent molecules to the nickel ion.

Keywords: nickel · redox chemistry · solvatochromism · substituent effects · thermochromism

Introduction

Transition-metal complexes containing redox-active dioxolene ligands, represented as quinone (Q), semiquinone (SQ), and catecholate (Cat), have been one of the most important and attractive research objectives, since they exhibit unusual valence tautomeric interconversion.[1] Valence tautomers are characterized by different distributions of electron density such as M^{II}-SQ and M^{III}-Cat compounds (M: metal ion), which interconvert to each other through intramolecular electron transfer between metal and ligand centers.

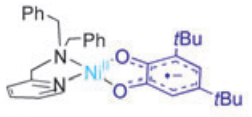

$[Ni^{II}(Py(Bz)_2)(tBu_2SQ)](PF_6)$ (**1**)

$[Ni^{III}(MePy(Bz)_2)(tBu_2Cat)](PF_6)$ (**2**)

Much information about metal complexes with dioxolene[2–4] and other redox-active ligands[5–8] exhibiting valence tautomeric behavior has been accumulated and this phenomenon has been explored in order to develop molecular switching devices.[9] However, nickel–dioxolene complexes that exhibit valence tautomeric interconversion have not been reported, and there has so far been no experiments to control the valence tautomerism taking advantage of the donor ability of the ligands[10] and external perturbation.

A pivotal property of nickel(II) complexes[11–16] is that they exhibit the unique solvatochromism and thermochromism induced by the transformation of the nickel(II) spin state between a low-spin ($S=0$) state with a tetracoordinate square-planar structure and a high-spin ($S=1$) state with a hexacoordinate octahedral geometry,[17,18] triggered by the coordination of two solvent molecules to the nickel ion. The importance of control over nickel(II) spin states has recognized not only in inorganic chemistry,[17–20] but also in biological chemistry,[21,22] since it promotes the development of molecular memories and switches[9,17–20] as well as leading to further understanding of biological systems.[21,22] In this context, we have recently demonstrated that modulation of the donor ability of the ligands in nickel(II) complexes makes it possible to control the spin states between $S=0$ and $S=1$.[23] This finding stimulated us to research the effect of the spin-

[a] Dr. H. Ohtsu, Prof. K. Tanaka
Institute for Molecular Science
CREST, Japan Science and Technology Agency (JST)
5–1 Higashiyama, Myodaiji, Okazaki, Aichi 444–8787 (Japan)
Fax: (+81) 564-59-5582
E-mail: ktanaka@ims.ac.jp

Supporting information for this article is available on the WWW under http://www.chemeurj.org/ or from the author.

DOI: 10.1002/chem.200500068

state change in valence tautomeric compounds containing nickel ions.

We report herein the synthesis, XPS, EPR, and electronic spectroscopic investigations of tetracoordinate square-planar low-spin nickel(II)–semiquinonato and nickel(III)–catecholato complexes that contain bidentate ligands with modulated nitrogen donor ability, $Py(Bz)_2$ or $MePy(Bz)_2$ {$Py(Bz)_2$ = *N*,*N*-bis(benzyl)-*N*-[(2-pyridyl)methyl]amine, $MePy(Bz)_2$ = *N*,*N*-bis(benzyl)-*N*-[(6-methyl-2-pyridyl)methyl]amine},[24] represented as $[Ni^{II}(Py(Bz)_2)(tBu_2SQ)](PF_6)$ (**1**) and $[Ni^{III}(MePy(Bz)_2)(tBu_2Cat)](PF_6)$ (**2**) (tBu_2SQ = 3,5-di-*tert*-butyl-1,2-benzosemiquinone, tBu_2Cat = 3,5-di-*tert*-butylcatecholate). In this article, we have two goals. The first is to report

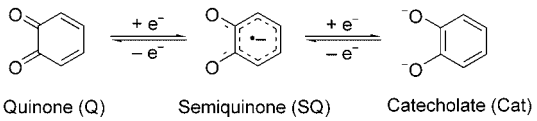

the first example for successful control of the Ni^{II}-SQ and Ni^{III}-Cat frameworks through fine-tuning of nitrogen donor ability of the bidentate ligands to the nickel ion. The second is to clarify the drastic difference in the solvent- and temperature-dependent interconversion processes of **1** and **2**; the transformation between square-planar low-spin Ni^{II}-SQ and octahedral high-spin Ni^{II}-SQ states occurs in **1**, whereas square-planar low-spin Ni^{III}-Cat framework is transformed to octahedral high-spin Ni^{II}-SQ states in the case of **2**.

Results and Discussion

Preparation and characterization of the nickel(II)–semiquinonato and nickel(III)–catecholato complexes: The reactants $Py(Bz)_2$, tBu_2CatH_2, and $Ni(ClO_4)_2{\cdot}6H_2O$ were mixed in a 1:1:1 ratio in acetonitrile under a nitrogen atmosphere, and then two equivalents of triethylamine and one equivalent of ferricenium hexafluorophosphate were added to the resulting solution. This procedure enabled us to isolate the nickel(II)–semiquinonato complex **1**. In the same manner, the nickel(III)–catecholato complex **2** was obtained using the $MePy(Bz)_2$ ligand instead of $Py(Bz)_2$ (see Experimental Section). The colors of both complexes are entirely different, since **1** is blue, whereas **2** is brown.

The oxidation states of the nickel ions in **1** and **2** were determined by X-ray photoelectron spectra (XPS). The XPS of **1** and **2** are shown in Figure 1 (parts a and b, respectively). The binding energy of the Ni $2p_{3/2}$ signals are observed at 854.9 (for **1**) and 856.1 eV (for **2**). The Ni $2p_{3/2}$ peak in **2** is evidently higher than that in **1**, a fact which reveals the nickel oxidation states in **1** and **2** are Ni^{II} and Ni^{III}, respectively.[25] Such a result is consistent with the EPR studies, as described below.

The EPR spectrum of **1** in dichloromethane (CH_2Cl_2) at 193 K is shown in Figure 2, which exhibits a sharp isotropic

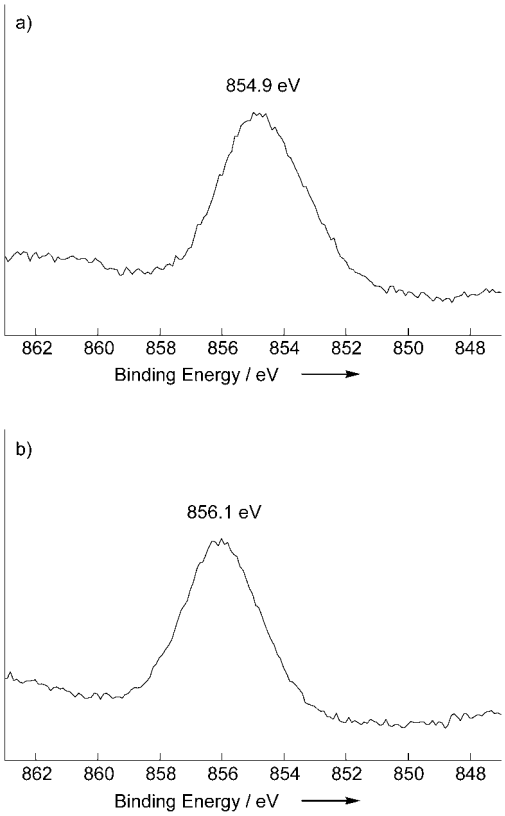

Figure 1. X-ray photoelectron spectra of a) $[Ni^{II}(Py(Bz)_2)(tBu_2SQ)](PF_6)$ (**1**) and b) $[Ni^{III}(MePy(Bz)_2)(tBu_2Cat)](PF_6)$ (**2**).

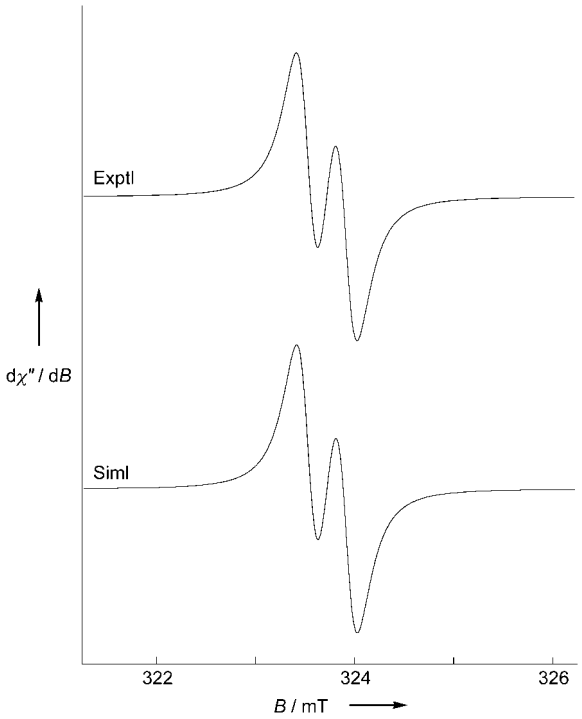

Figure 2. EPR spectrum of $[Ni^{II}(Py(Bz)_2)(tBu_2SQ)](PF_6)$ (**1**) (1.0×10^{-3} M) in CH_2Cl_2 at 193 K, and its computer simulation using the parameters (g = 2.0061, a_H = 0.38 mT).

signal at $g=2.0061$ with hyperfine structure.[26] The hyperfine coupling constant was determined by the computer simulation of the EPR spectrum as shown in Figure 2. The two-line isotropic signal is ascribed to the hyperfine coupling ($a_H=0.38$ mT) of an unpaired electron with the proton in the 4-position of the dioxolene ligand.[27] The observed sharp isotropic signal with the g value of 2.0061 is close to free-spin value ($g=2.0023$) and can be assigned to the ligand-centered radical species consisted of the square-planar low-spin d^8 Ni^{II} ($S=0$) and semiquinone radical ($S=1/2$) frameworks.

In contrast to **1**, interestingly, an anisotropic signal ($g_\perp=2.29$, $g_\parallel=2.20$, and $g_{iso}=2.26$)[28] is obtained at 77 K in the case of **2** (Figure 3). The significantly larger g value of **2**

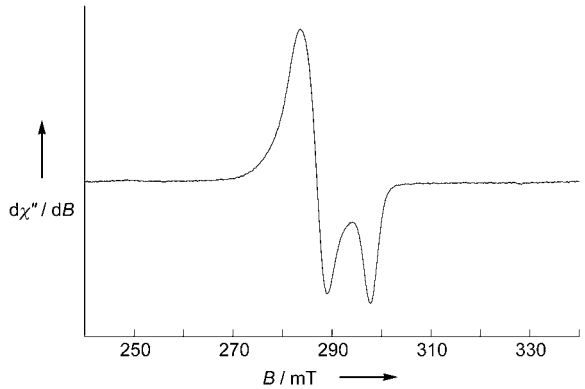

Figure 3. EPR spectrum of $[Ni^{III}(MePy(Bz)_2)(tBu_2Cat)](PF_6)$ (**2**) (1.0×10^{-3} M) in CH_2Cl_2 at 77 K.

($g_{iso}=2.26$) compared with that of **1** ($g=2.0061$) clearly indicates that the unpaired electron is localized on the metal center. The electronic configuration of **2** can thus be interpreted as metal-centered oxidized species composed of the low-spin d^7 Ni^{III} ($S=1/2$) and catecholate ($S=0$) states. Furthermore, the EPR parameters ($g_\perp=2.29$, $g_\parallel=2.20$) strongly indicate that the coordination environment of the nickel(III) ion is a distorted square-planar structure with a d_{z^2} ground state.[29]

The cyclic voltammograms of **1** and **2** have been measured in CH_2Cl_2 under anaerobic conditions and show two reversible redox waves (**1**: $E_{1/2a}=0.63$ V and $E_{1/2b}=0.19$ V, **2**: $E_{1/2a}=0.59$ V and $E_{1/2b}=0.10$ V vs SCE). Taking into account the results of XPS data (Ni $2p_{3/2}=854.9$ eV) as well as EPR signal ($g=2.0061$), the first $E_{1/2a}$ and the second $E_{1/2b}$ redox waves of **1** are assigned to the Ni^{III}/Ni^{II} couple and the Cat/SQ couple, respectively. On the other hand, the first and second reversible waves of **2** at $E_{1/2a}$ and $E_{1/2b}$ correspond to the SQ/Cat and Ni^{II}/Ni^{III} redox couples, respectively, based on the XPS (Ni $2p_{3/2}=856.1$ eV) and EPR ($g_{iso}=2.26$) measurements.

Such a drastic difference in the electronic states of **1** and **2** can be ascribed to the steric effect induced by the *o*-methyl group[23,30–32] in the $MePy(Bz)_2$ ligand. The *o*-methyl group of the $MePy(Bz)_2$ ligand leads to the weaker coordination to the nickel ion relative to the nonsubstituted $Py(Bz)_2$ ligand. As a result, the dioxolene ligand of **2** binds more strongly to the nickel ion than that observed for **1**; this causes the deviation of electron density to form the Ni^{II}-SQ and Ni^{III}-Cat states selectively.

The conformational changes to give octahedral structures from the square-planar nickel(II)–semiquinonato and nickel(III)–catecholato complexes: The addition of an exogenous ligand such as nitrate ion (NO_3^-) into a solution of the tetracoordinate square-planar low-spin nickel(II)–semiquinonato (**1**) or nickel(III)–catecholato (**2**) complexes in CH_2Cl_2 resulted in color changes from blue and brown, respectively, to light green. The absorption spectral changes observed upon addition of tetra-*n*-butylammonium nitrate (TBA-NO_3) into a solution of **1** or **2** in CH_2Cl_2 are shown in Figures 4 and 5, respectively. The absorption spectrum of blue **1** exhibits an intense band at 595 nm[33] ($\varepsilon=2500\,M^{-1}cm^{-1}$), which can be

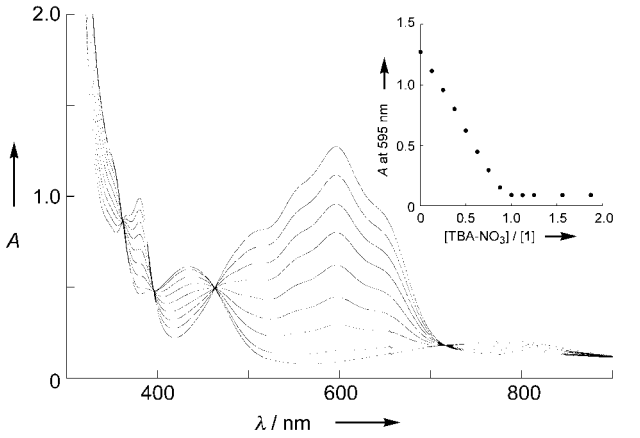

Figure 4. Absorption spectral changes observed upon addition of various amounts of TBA-NO_3 into a solution of $[Ni^{II}(Py(Bz)_2)(tBu_2SQ)](PF_6)$ (**1**) in CH_2Cl_2 (5.0×10^{-4} M) at 298 K. Inset: Titration of **1** with TBA-NO_3 in CH_2Cl_2 at 298 K.

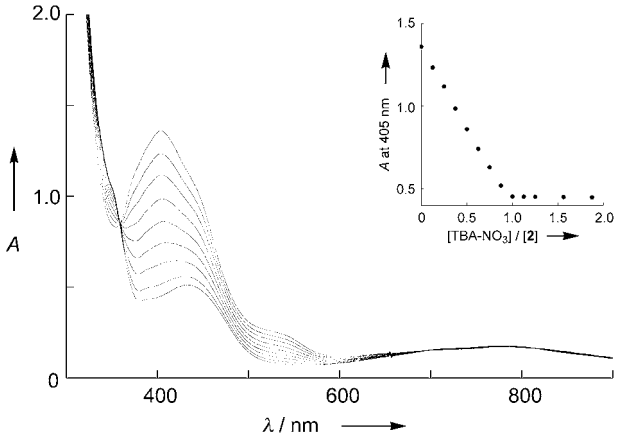

Figure 5. Absorption spectral changes observed upon addition of various amounts of TBA-NO_3 into a solution of $[Ni^{III}(MePy(Bz)_2)(tBu_2Cat)](PF_6)$ (**2**) in CH_2Cl_2 (5.0×10^{-4} M) at 298 K. Inset: Titration of **2** with TBA-NO_3 in CH_2Cl_2 at 298 K.

assigned to the charge-transfer transition between the semiquinone and the low-spin nickel(II) ion. The absorbance of the band at 595 nm decreases linearly with an increase in the NO_3^- concentration up to just one equivalent of NO_3^-. No other spectral change is observed even when an excess amount of NO_3^- is added as depicted in the inset of Figure 4. This result clearly indicates that the stoichiometry of the reaction between **1** and NO_3^- is 1:1. In the case of brown **2**, the absorption spectrum displays characteristic bands centered at 405, 540, and 775 nm[33] ($\varepsilon = 2700$, 450, and 350 $M^{-1}cm^{-1}$, respectively) associated with nickel(III) complexes.[34] The spectral change behavior in the reaction of **2** with NO_3^- (see the inset of Figure 5) is the same as that in **1**, and the spectrum of the resulting light green solution of **2** (λ_{max} (ε) = 435 (1200) and 785 nm (400 $M^{-1}cm^{-1}$)) is also quite close to that of **1** (λ_{max} (ε) = 435 (1000) and 780 nm (350 $M^{-1}cm^{-1}$)).

The EPR measurements allows us to clarify the electronic structures of the 1:1 adducts formed in the reaction between **1** or **2** and NO_3^-. The EPR spectra of the 1:1 NO_3^- adducts in **1** and **2**, denoted as complexes **3** and **4**, respectively, at 77 K are shown in Figure 6, from which the EPR parameters

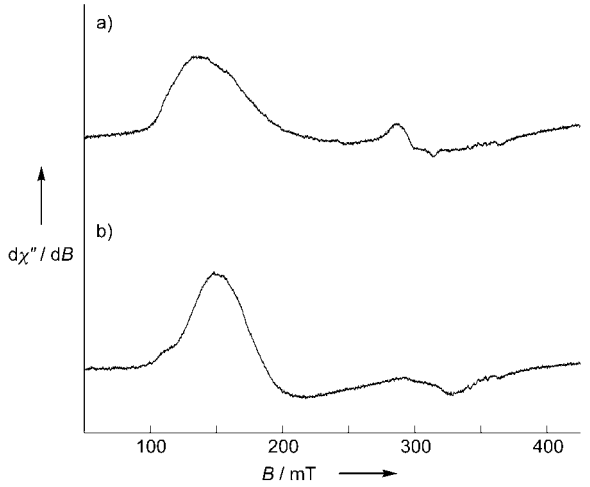

Figure 6. EPR spectra of a) $[Ni^{II}(Py(Bz)_2)(tBu_2SQ)(NO_3)]$ (**3**) (1.0×10^{-3} M) and b) $[Ni^{II}(MePy(Bz)_2)(tBu_2SQ)(NO_3)]$ (**4**) (1.0×10^{-3} M) in CH_2Cl_2 at 77 K.

($g_1 = 5.0$ and 4.6, $g_2 = 2.2$ and 2,1, $g_3 = 1.9$ and 1.9 for **3** and **4**, respectively)[28] are obtained. Such EPR signals in both complexes at X-band frequency are typical of a Kramers' doublet in a quartet ground state and clearly indicate that the nickel(II) ion with the high-spin state ($S = 1$) is ferromagnetically coupled to the semiquinone radical ($S = 1/2$) to yield a total $S = 3/2$ state.[35,36] Furthermore, the oxidation states of nickel ion in both 1:1 NO_3^- adducts has been confirmed by XPS. The detected binding energy of the Ni $2p_{3/2}$ signals at 855.3 eV (for both complexes) are consistent with the Ni^{II} oxidation states.[25] Thus, the electronic structures of the 1:1 adducts with NO_3^- in **1** and **2** can be expressed as the hexacoordinate octahedral high-spin Ni^{II}-SQ complexes, $[Ni^{II}(Py(Bz)_2)(tBu_2SQ)(NO_3)]$ (**3**) and $[Ni^{II}(MePy(Bz)_2)(tBu_2SQ)(NO_3)]$ (**4**)[37] (Scheme 1). Indeed, the observed EPR and absorption spectra are the same as those of the structurally established hexacoordinate octahedral high-spin nickel(II)–semiquinonato complex.[35] Such color changes induced by the transformation from square-planar low-spin Ni^{II}-SQ and Ni^{III}-Cat complexes to the octahedral high-spin Ni^{II}-SQ complexes occur when either noncoordinating or coordinating solvents are used.

Solvatochromic and thermochromic behavior: The characteristic absorption bands of tetracoordinate square-planar low-spin Ni^{II}-SQ and Ni^{III}-Cat complexes (**1**: $\lambda = 595$ nm ($\varepsilon = 2500\ M^{-1}cm^{-1}$), **2**: $\lambda = 405$, 540, and 775 nm ($\varepsilon = 2700$, 450, and 350 $M^{-1}cm^{-1}$, respectively)) are observed in CH_2Cl_2, a noncoordinating solvent, as described above. The spectra of **1** and **2**, however, completely change when a coordinating solvent such as tetrahydrofuran (THF) is used instead of CH_2Cl_2. The obtained absorption bands of **1** and **2** in THF are centered at $\lambda = 425$ ($\varepsilon = 1200$), 795 nm ($\varepsilon = 350\ M^{-1}cm^{-1}$) and $\lambda = 420$ ($\varepsilon = 850$), 790 nm ($\varepsilon = 350\ M^{-1}cm^{-1}$), respectively, and are very close to those of the 1:1 NO_3^- adducts **3** and **4** as shown in Figure 4 and 5. In addition, the EPR spectra of **1** and **2** in THF at 77 K (**1**: $g = 4.7$, 2.1, 1.9, **2**: $g = 5.0$, 2.1, 1.9; see Supporting Information)[28] are exactly the same as those of **3** and **4** (see Figure 6). These results indicate that the conversion from square-planar low-spin Ni^{II}-SQ and Ni^{III}-Cat complexes to octahedral high-spin Ni^{II}-SQ complexes is attributable to the coordination of two THF molecules to the tetracoordinate square-planar nickel center. Formation of the 1:2 solvent molecule adducts has been further confirmed by the CSI mass spectrum of **1** in *N*,*N*-dimethylformamide (DMF), which is a also a coordinating solvent like THF. A signal at *m/z* 712 was exhibited and the observed mass and isotope pattern correspond to the ion $[Ni^{II}(Py(Bz)_2)(tBu_2SQ)(dmf)_2]^+$.

As expected from the solvatochromic properties of **1** and **2**, the conversion of square-planar low-spin Ni^{II}-SQ and

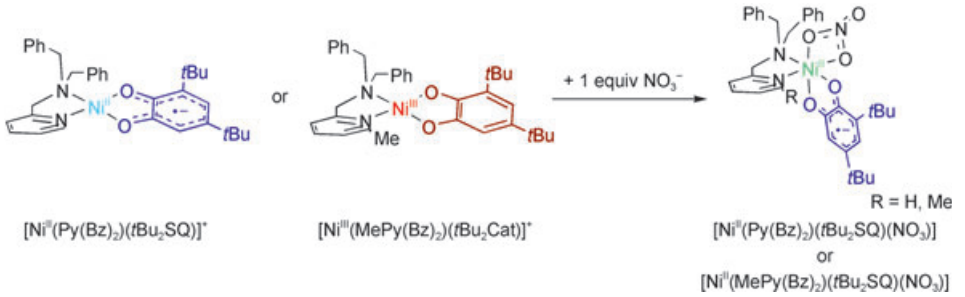

Scheme 1.

Ni^{III}-Cat complexes to octahedral high-spin Ni^{II}-SQ complexes can be induced by gradual addition of DMF into a solution of **1** or **2** in CH_2Cl_2 (Figure 7). The characteristic

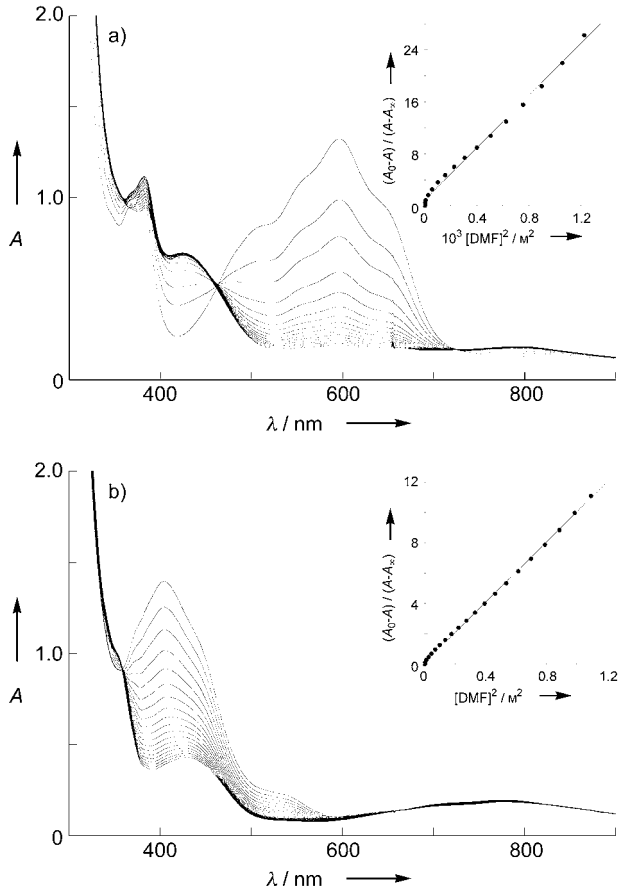

Figure 7. Absorption spectral changes observed upon addition of various amounts of DMF into a solution of a) $[Ni^{II}(Py(Bz)_2)(tBu_2SQ)](PF_6)$ (**1**) in CH_2Cl_2 (5.0×10^{-4} M) and b) $[Ni^{III}(MePy(Bz)_2)(tBu_2Cat)](PF_6)$ (**2**) in CH_2Cl_2 (5.0×10^{-4} M) at 298 K. Insets: Plots of $(A_0-A)/(A-A_\infty)$ versus $[DMF]^2$ for the 1:2 DMF adducts of a) **1** and b) **2**.

absorption bands at $\lambda=595$ (for **1**) and 405 nm (for **2**) decrease with increasing the concentration of added DMF, accompanied by increases in the absorption bands at ~430 and ~800 nm in both cases, which belong to the corresponding octahedral high-spin Ni^{II}–DMF adducts. Such absorption spectral changes shown in Figure 7 are reasonably associated with the 1:2 complex formation between **1** or **2** and DMF as illustrated in Scheme 2.[38] The binding constants (K_b) for the 1:2 adducts with DMF expressed by [Eq. (1)] were calculated by using the equation $(A_0-A)/(A-A_\infty)=K_b[DMF]^2$.

$$K_b = \frac{[Ni^{II}(Py(Bz)_2 \text{ or } MePy(Bz)_2)(tBu_2SQ)(dmf)_2]}{[Ni^{II}(Py(Bz)_2)(tBu_2SQ) \text{ or } Ni^{III}(MePy(Bz)_2)(tBu_2Cat)][DMF]^2} \quad (1)$$

The plots of $(A_0-A)/(A-A_\infty)$ versus $[DMF]^2$ give straight lines passing through the origin as shown in the insets of Figure 7. The K_b values are determined as 2.0×10^4 and $9.9\,M^{-2}$ for **1** and **2**, respectively, from the slopes of the plots. The significantly larger binding constant of **1** with respect to that of **2** may be due to the difference in the interconversion processes of **1** and **2**. In complex **1** only the nickel(II) spin states, such as low- and high-spin Ni^{II}-SQ, are transformed, whereas in complex **2** the conversion of low-spin Ni^{III}-Cat and high-spin Ni^{II}-SQ states occurs, as depicted in Scheme 2. Such a drastic difference of K_b values in **1** and **2** has an influence to the thermal behavior of both complexes.

The tetracoordinate square-planar low-spin Ni^{II}-SQ complex, $[Ni^{II}(Py(Bz)_2)(tBu_2SQ)]^+$ (**1**), exhibits reversible thermochromism induced by the nickel(II) spin-state interconversion between square-planar low-spin and octahedral high-spin states with the SQ ligand when 2.5 equivalents of DMF are added to a solution of **1** in CH_2Cl_2 (see Supporting Information). At room temperature, there is a band ($\lambda_{max}=$ 595 nm) that is characteristic of the low-spin Ni^{II}-SQ form. As the temperature of this blue solution of **1** is decreased from 298 K to 213 K, the color gradually changes toward light green ($\lambda_{max}=425$ and 795 nm) very similar to the spectrum with in one equivalent of TBA-NO_3 (Figure 4) and that with excess amounts of DMF in CH_2Cl_2 (Figure 7a). The notable thermochromism can be explained by the shift of the equilibrium to the right upon cooling the solution down to 213 K as shown in Scheme 2.

In contrast to the case of **1**, temperature-dependent spectral change is not observed under the same conditions for complex **2** (2.5 equiv of DMF). On the other hand, when 200 equivalents of DMF are added to a solution of **2** in CH_2Cl_2, the thermochromism between two distinguishable electronic isomers, one is low-spin $[Ni^{III}(MePy(Bz)_2)(tBu_2Cat)]^+$ with square-planar structure (brown) and the other is high-spin $[Ni^{II}(MePy(Bz)_2)(tBu_2SQ)(dmf)_2]^+$ with octahedral geometry (light green), takes place as illustrated in Scheme 2 (see also the Supporting Information). Such a

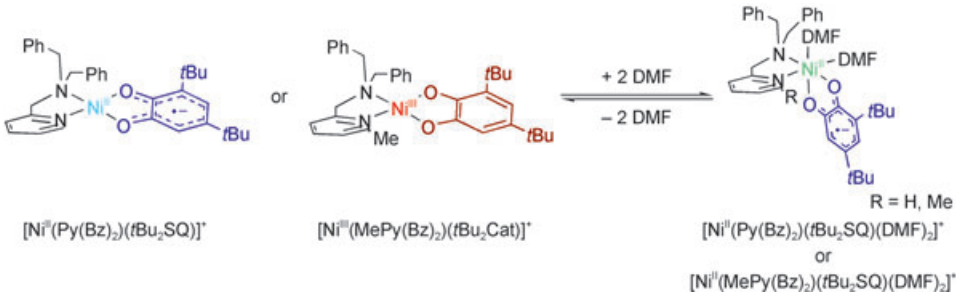

Scheme 2.

difference in the amounts of DMF to cause the thermochromism is associated with the binding constants of **1** ($K_b = 2.0\times10^4\,M^{-2}$) and **2** ($K_b = 9.9\,M^{-2}$) with DMF (vide supra). Thus, the modulation of nitrogen-donor ability of the bidentate ligands plays a crucial role in controlling thermochromism as well as solvatochromism in conjunction with electronic distribution.

Conclusion

The tetracoordinate square-planar low-spin nickel(II)–semiquinonato and nickel(III)–catecholato complexes, $[Ni^{II}(Py(Bz)_2)(tBu_2SQ)](PF_6)$ (**1**) and $[Ni^{III}(MePy(Bz)_2)(tBu_2Cat)](PF_6)$ (**2**), have been synthesized selectively by using bidentate ligands with modulated nitrogen-donor ability to the nickel ion. Complexes **1** and **2** exhibit the unique solvatochromism as well as thermochromism induced by electronic structural changes between square-planar low-spin Ni^{II}-SQ (blue) or Ni^{III}-Cat (brown) and octahedral high-spin Ni^{II}-SQ (light green) states. The significantly larger binding constant of **1** ($K_b = 2.0\times10^4\,M^{-2}$) for the 1:2 DMF adducts with respect to that of **2** ($K_b = 9.9\,M^{-2}$) and the thermochromic condition (**1**: 2.5 equiv of DMF, **2**: 200 equiv of DMF) may be caused by the different interconversion pathways in **1** and **2**. Complex **1** is transformed between square-planar low-spin Ni^{II}-SQ ($[Ni^{II}(Py(Bz)_2)(tBu_2SQ)]^+$) and octahedral high-spin Ni^{II}-SQ ($[Ni^{II}(Py(Bz)_2)(tBu_2SQ)(dmf)_2]^+$), whereas complex **2** converts between square-planar low-spin Ni^{III}-Cat ($[Ni^{III}(MePy(Bz)_2)(tBu_2Cat)]^+$) and octahedral high-spin Ni^{II}-SQ ($[Ni^{II}(MePy(Bz)_2)(tBu_2SQ)(dmf)_2]^+$). Thus, control of valence distribution in the nickel–dioxolene system can be accomplished by fine-tuning of the donor ability of the bidentate ligands to the nickel ion as well as solvent and thermal effects.

Experimental Section

Materials: All chemicals used for the synthesis of the ligands and complexes were commercial products of the highest available purity and were further purified by the standard methods.[39] Solvents were also purified by standard methods before use.[39]

Synthesis: All ligands and complexes used in this study were prepared according to the following procedures and the structures of the products were confirmed by the analytical data (vide infra).

***N,N*-Bis(benzyl)-*N*-[(2-pyridyl)methyl]amine ($Py(Bz)_2$) and *N,N*-bis(benzyl)-*N*-[(6-methyl-2-pyridyl)methyl]amine ($MePy(Bz)_2$):** These ligands used in this study were prepared as described previously.[24]

$[Ni^{II}(Py(Bz)_2)(tBu_2SQ)](PF_6)$ (1): $Ni(ClO_4)_2\cdot6H_2O$ (0.366 g, 1.0 mmol) in acetonitrile (10 mL) was added to a solution of $Py(Bz)_2$ (0.288 g, 1.0 mmol) and tBu_2CatH_2 (0.222 g, 1.0 mmol) in acetonitrile (10 mL) under a nitrogen atmosphere, followed by addition of triethylamine (0.202 g, 2.0 mmol). The ferricenium hexafluorophosphate (0.331 g, 1.0 mmol) was added to the mixture, and the solution was stirred for 2 h at room temperature. After removal of the solvent under reduced pressure, the resulting residue was dissolved in dichloromethane and ammonium hexafluorophosphate (0.326 g, 2.0 mmol) was added to the solution. The mixture was stirred overnight at room temperature, and insoluble material was removed by filtration. Addition of pentane to the filtrate gradually gave blue powder that was collected by filtration and recrystallized from dichloromethane/pentane. Yield: 0.380 g (53.4%); ESI MS data: *m/z*: 566 $[M-PF_6]^+$; elemental analysis calcd (%) for $C_{34}H_{40}F_6N_2O_2Ni_1P_1$: C 57.33, H 5.66, N 3.93; found: C 57.14, H 5.62, N 3.90.

$[Ni^{III}(MePy(Bz)_2)(tBu_2Cat)](PF_6)$ (2): This complex, the color of which is brown, was prepared in the same manner as that for the synthesis of **1** but with the $MePy(Bz)_2$ ligand instead of $Py(Bz)_2$. Yield: 0.259 g (35.7%); ESI MS data: *m/z*: 580 $[M-PF_6]^+$; elemental analysis calcd (%) for $C_{36}H_{43.5}F_6N_{2.5}O_2Ni_1P_1$: C 57.89, H 5.87, N 4.69; found: C 57.63, H 6.04, N 4.51.

Measurements: NMR measurements were performed with a JEOL GX-500 (500 MHz) NMR spectrometer. Electronic spectra were measured with a Hewlett-Packard 8453 diode array spectrophotometer with a Unisoku thermostated cell holder designed for low-temperature experiments. Solution and frozen solution EPR spectra were taken on a JEOL JES-FA200 equipped with an attached VT (variable temperature) apparatus and were recorded under nonsaturating microwave power conditions. The magnitude of the modulation was chosen to optimize the resolution and the signal-to-noise ratio of the observed spectra. The *g* values were calibrated with a Mn^{II} marker used as a reference. XPS (X-ray photoelectron spectra) were recorded on a VG Scientific Ltd. ESCALAB 220i-XL. Mg Kα radiation (1253.6 eV) operated at 15 kV and 20 mA was used as an X-ray excitation source. All samples were deposited on gold foil from solutions of the sample in CH_2Cl_2. The C1s peak was assigned as the value of 284.6 eV and used as the internal reference. ESI-mass spectra were obtained with a Shimadzu LCMS-2010 liquid chromatograph mass spectrometer. CSI (cold-spray ionization) mass spectra were taken on a JEOL JMS-T100CS attached to a syringe pump apparatus (Harvard Apparatus model 22). Sample solutions were delivered to the sprayer through a fused silica capillary (100 μm diameter) at 10 $\mu L\,s^{-1}$. The sprayer was held at a potential of 2.0 kV, and compressed N_2 controlled the temperature at 248 K was employed to assist liquid nebulization. The orifice potential was maintained at 30 V. The positive ion CSI-mass spectra were measured in the range of *m/z* 100 to 1000. Cyclic voltammetry measurements were performed at 298 K on an ALS/Chi model 660 electrochemical analyzer in deaerated solvent containing 0.1 M tetra-*n*-butylammonium hexafluorophosphate (TBA-PF_6) as a supporting electrolyte. A conventional three-electrode cell was used with a glassy-carbon working electrode and a platinum wire as the counter electrode. The glassy-carbon working electrode was routinely polished with a BAS polishing alumina suspension and rinsed with acetone before use. The reversibility of the electrochemical processes were evaluated by standard procedures and all potentials were recorded against an SCE reference electrode, which was calibrated by using the ferrocene/ferricenium redox couple. All electrochemical measurements were carried out under an atmospheric pressure of argon. Elemental analyses were carried out at Research Center for Molecular-scale Nanoscience, Institute for Molecular Science.

Acknowledgements

We are grateful to Prof. Toshihiko Yokoyama and Dr. Takeshi Nakagawa, Institute for Molecular Science, for the measurements of X-ray photoelectron spectra and JEOL ltd. for measuring CSI-mass spectra.

[1] a) C. G. Pierpont, R. M. Buchanan, *Coord. Chem. Rev.* **1981**, *38*, 45–87; b) C. G. Pierpont, C. W. Lange, *Prog. Inorg. Chem.* **1994**, *41*, 331–442; c) C. G. Pierpont, *Coord. Chem. Rev.* **2001**, *216/217*, 99–125.

[2] a) G. A. Abakumov, G. A. Razuvaev, V. I. Nevodchikov, V. K. Cherkasov, *J. Organomet. Chem.* **1988**, *341*, 485–494; b) C. Roux, D. M. Adams, J. P. Itie, A. Polian, D. N. Hendrickson M. Verdaguer, *Inorg. Chem.* **1996**, *35*, 2846–2852; c) P. Gütlich, A. Dei, *Angew. Chem.* **1997**, *109*, 2852–2855; *Angew. Chem. Int. Ed. Engl.* **1997**, *36*, 2734–2736; d) J. Rall, M. Wanner, M. Albrecht, F. M. Hornung, W. Kaim,

Chem. Eur. J. **1999**, *5*, 2802–2809; e) C. Carbonera, A. Dei, J.-F. Létard, C. Sangregorio, L. Sorace, *Angew. Chem.* **2004**, *116*, 3198–3200; *Angew. Chem. Int. Ed.* **2004**, *43*, 3136–3138.
[3] a) R. M. Buchanan, C. G. Pierpont, *J. Am. Chem. Soc.* **1980**, *102*, 4951–4957; b) A. S. Attia, C. G. Pierpont, *Inorg. Chem.* **1995**, *34*, 1172–1179; c) O.-S. Jung, D. H. Jo, Y.-A. Lee, Y. S. Sohn, C. G. Pierpont, *Angew. Chem.* **1996**, *108*, 1796–1797; *Angew. Chem. Int. Ed. Engl.* **1996**, *35*, 1694–1695; d) C. W. Lange, C. G. Pierpont, *Inorg. Chim. Acta* **1997**, *263*, 219–224; e) O.-S. Jung, D. H. Jo, Y.-A. Lee, B. J. Conklin, C. G. Pierpont, *Inorg. Chem.* **1997**, *36*, 19–24.
[4] a) D. M. Adams, A. Dei, A. L. Rheingold, D. N. Hendrickson, *J. Am. Chem. Soc.* **1993**, *115*, 8221–8229; b) D. M. Adams, B. Li, J. D. Simon, D. N. Hendrickson, *Angew. Chem.* **1995**, *107*, 1580–1582; *Angew. Chem. Int. Ed. Engl.* **1995**, *34*, 1481–1483; c) D. Ruiz, J. Yoo, I. A. Guzei, A. L. Rheingold, D. N. Hendrickson, *Chem. Commun.* **1998**, 2089–2090; d) D. Ruiz-Molina, L. N. Zakharov, A. L. Rheingold, D. N. Hendrickson, *J. Phys. Chem. Solids* **2004**, *65*, 831–837.
[5] F. V. Lovecchio, E. S. Gore, D. H. Busch, *J. Am. Chem. Soc.* **1974**, *96*, 3109–3118.
[6] J. Seth, V. Palaniappan, D. F. Bocian, *Inorg. Chem.* **1995**, *34*, 2201–2206.
[7] Y. Shimazaki, F. Tani, K. Fukui, Y. Naruta, O. Yamauchi, *J. Am. Chem. Soc.* **2003**, *125*, 10512–10513.
[8] I. Ratera, D. Ruiz-Molina, F. Renz, J. Ensling, K. Wurst, C. Rovira, P. Gütlich, J. Veciana, *J. Am. Chem. Soc.* **2003**, *125*, 1462–1463.
[9] a) O. Kahn, J. P. Launay, *Chemtronics* **1988**, *3*, 140–151; b) O. Kahn, J. Kröber, C. Jay, *Adv. Mater.* **1992**, *4*, 718–728.
[10] For a preliminary report, see: H. Ohtsu, K. Tanaka, *Angew. Chem.* **2004**, *116*, 6461–6463; *Angew. Chem. Int. Ed.* **2004**, *43*, 6301–6303.
[11] a) Y. Ihara, R. Tsuchiya, *Bull. Chem. Soc. Jpn.* **1980**, *53*, 1614–1617; b) Y. Ihara, E. Izumi, A. Uehara, R. Tsuchiya, S. Nakagawa, E. Kyuno, *Bull. Chem. Soc. Jpn.* **1982**, *55*, 1028–1032; c) Y. Ihara, R. Tsuchiya, *Bull. Chem. Soc. Jpn.* **1984**, *57*, 2829–2831; d) Y. Ihara, *Bull. Chem. Soc. Jpn.* **1985**, *58*, 3248–3251; e) Y. Ihara, A. Wada, Y. Fukuda, K. Sone, *Bull. Chem. Soc. Jpn.* **1986**, *59*, 2309–2315; f) Y. Ihara, Y. Fukuda, K. Sone, *Inorg. Chem.* **1987**, *26*, 3745–3750.
[12] Y. Fukuda, K. Sone, *J. Inorg. Nucl. Chem.* **1972**, *34*, 2315–2328.
[13] J. D. Vitiello, E. J. Billo, *Inorg. Chem.* **1980**, *19*, 3477–3481.
[14] a) R. W. Hay, R. Bembi, W. Sommerville, *Inorg. Chim. Acta* **1982**, *59*, 147–153; b) R. W. Hay, B. Jeragh, G. Ferguson, B. Kaitner, B. L. Ruhl, *J. Chem. Soc. Dalton Trans.* **1982**, 1531–1539.
[15] I. R. Laskar, T. K. Maji, D. Das, T.-H. Lu, W.-T. Wong, K. Okamoto, N. R. Chaudhuri, *Polyhedron* **2001**, *20*, 2073–2082.
[16] A. Flamini, V. Fares, A. Pifferi, *Eur. J. Inorg. Chem.* **2000**, 537–544.
[17] D. R. Bloomquist, R. D. Willett, *Coord. Chem. Rev.* **1982**, *47*, 125–164.
[18] K. Sone, Y. Fukuda, *Inorganic Thermochromism*, Springer, Berlin, **1987**.
[19] H. Toftlund, *Coord. Chem. Rev.* **1989**, *94*, 67–128.
[20] a) P. Gütlich, A. Hauser, H. Spiering, *Angew. Chem.* **1994**, *106*, 2109–2141; *Angew. Chem. Int. Ed. Engl.* **1994**, *33*, 2024–2054; b) P. Gütlich, Y. Garcia, H. A. Goodwion, *Chem. Soc. Rev.* **2000**, *29*, 419–427; c) P. Gütlich, Y. Garcia, T. Woike, *Coord. Chem. Rev.* **2001**, *219–221*, 839–879.
[21] a) M. M. Maltempo, *J. Chem. Phys.* **1974**, *61*, 2540–2547; b) M. M. Maltempo, T. H. Moss, M. A. Cusanovich, *Biochim. Biophys. Acta* **1974**, *342*, 290–305.
[22] S. Fujii, T. Yoshimura, H. Kamada, K. Yamaguchi, S. Suzuki, S. Shidara, S. Takakuwa, *Biochim. Biophys. Acta* **1995**, *1251*, 161–169.
[23] H. Ohtsu, K. Tanaka, *Inorg. Chem.* **2004**, *43*, 3024–3030.
[24] Y. Shimazaki, T. Nogami, F. Tani, A. Odani, O. Yamauchi, *Angew. Chem.* **2001**, *113*, 3977–3980; *Angew. Chem. Int. Ed.* **2001**, *40*, 3859–3862.
[25] A. Davidson, J. F. Tempere, M. Che, *J. Phys. Chem.* **1996**, *100*, 4919–4929.
[26] The *g* value in the EPR spectrum was independent of temperature down to 4.2 K. However, hyperfine structure owing to the proton of the dioxolene ligand in the 4-position was not observed in a frozen medium, even at a much smaller modulation. This could be due to the fact that the hyperfine coupling constant may be too small to detect with the line width in frozen condition.
[27] J. J. Conradi, G. A. Maclaren, *J. Am. Chem. Soc.* **1960**, *82*, 4745.
[28] The EPR spectrum was practically independent of temperature down to 4.2 K.
[29] T. J. Collins, T. R. Nichols, E. S. Uffelman, *J. Am. Chem. Soc.* **1991**, *113*, 4708–4709.
[30] H. Nagao, N. Komeda, M. Mukaida, M. Suzuki, K. Tanaka, *Inorg. Chem.* **1996**, *35*, 6809–6815.
[31] Y. Shimazaki, S. Huth, S. Hirota, O. Yamauchi, *Bull. Chem. Soc. Jpn.* **2000**, *73*, 1187–1195.
[32] a) H. Ohtsu, Y. Shimazaki, A. Odani, O. Yamauchi, S. Itoh, S. Fukuzumi, *J. Am. Chem. Soc.* **2000**, *122*, 5733–5741; b) H. Ohtsu, S. Itoh, S. Nagatomo, T. Kitagawa, S. Ogo, Y. Watanabe, S. Fukuzumi, *Inorg. Chem.* **2001**, *40*, 3200–3207; c) H. Ohtsu, S. Fukuzumi, *Chem. Lett.* **2001**, *30*, 920–921.
[33] The reflectance spectrum in the solid state showed the same band, which indicates the structure is maintained in the solution state.
[34] R. I. Haines, A. Mcauley, *Coord. Chem. Rev.* **1981**, *39*, 77–119.
[35] C. Benelli, A. Dei, D. Gatteschi, L. Pardi, *Inorg. Chem.* **1988**, *27*, 2831–2836.
[36] J. Müller, A. Kikuchi, E. Bill, T. Weyhermüller, P. Hidebrandt, L. Ould-Moussa, K. Wieghardt, *Inorg. Chim. Acta* **2000**, *297*, 265–277.
[37] The binding mode of nitrate ion in **3** and **4**, which is bidentate, has been confirmed by infrared spectra; see: A. B. P. Lever, E. Mantovani, B. S. Ramaswamy, *Can. J. Chem.* **1971**, *49*, 1957–1964.
[38] The octahedral diaqua-complex, $[Ni^{II}(en)_2(H_2O)_2]^{2+}$ (en = ethylenediamine), favors the *cis* configuration as compared to the *trans* one in the solution state; see: M. E. Farago, J. M. James, V. C. G. Trew, *J. Chem. Soc. A* **1967**, 820–824. In the case of the 1:2 DMF adducts with **1** and **2**, the type of coordination has yet to be determined.
[39] D. D. Perrin, W. L. F. Armarego in *Purification of Laboratory Chemicals*, Butterworth-Heinemann, Oxford, **1988**.

Received: January 19, 2005
Published online: April 8, 2005